Localization in $Cr_{1-x}Fe_x$ amorphous films

1996 J. Phys.: Condens. Matter 8 11121

(http://iopscience.iop.org/0953-8984/8/50/035)

J. Phys.: Condens. Matter **8** (1996) 11121–11130. Printed in the UK

Localization in $Cr_{1-x}Fe_x$ amorphous films

Y Öner†, A Kiliç‡, M Özdemir§, H Çelik‖ and S Senoussi¶

† Department of Physics, Istanbul Technical University, 80626, Maslak, Istanbul, Turkey
‡ Department of Physics, University of Karaelmas, Zonguldak, Turkey
§ Department of Physics, University of Marmara, Istanbul, Turkey
‖ Department of Physics, University of Hacettepe, Ankara, Turkey
¶ Laboratoire de Physique des Solides (associe au CNRS), Université de Paris-Sud, Orsay Cédex, France

Received 21 May 1996

Abstract. The electrical resistivity has been measured as a function of temperature between 1.5–300 K for amorphous $Cr_{1-x}Fe_x$ alloys with $x = 0.176, 0.22, 0.26$. The resistivities all show square-root temperature dependences below the minima temperatures. The high-field magnetoresistance (H varies between 0–120 kOe) can be accounted for in theoretical models of localization in the presence of strong spin–orbit interaction. In addition, the spin-flip scattering rate due to local spin fluctuations decreases with increasing temperature and then levels off at about $T = 50$ K in a manner consistent with the magnetic state of the sample, while the inelastic scattering rate in this range remains almost of the same order. Furthermore, the magnetic anisotropy of the resistivity together with the magnetization data show that the magnetic order is progressively suppressed with increasing Fe content.

1. Introduction

Crystalline $Cr_{1-x}Fe_x$ alloys are known to have an interesting magnetic phase diagram [1]. For Fe concentration $x < 0.16$, there is an antiferromagnetic spin-density-wave order with a crossover from incommensurate to commensurate above $x \simeq 0.023$, an intermediate spin-glass phase in the narrow range $0.16 < x < 0.19$ and a re-entrant sequence in the range $0.19 < x < 0.25$, following the ferromagnetic phase for most of the range of $x > 0.25$. The small chromium moment disappears at around $x = 0.17$; iron retains a well-defined moment of approximately $2\mu_B$ over almost the entire range of the solid solution. However, glassy $(Cr_{1-x}Fe_x)M_y$ (M is a metalloid atom) alloys stabilized with about 20% of metalloid atoms present a rather different picture [2–5]. The Curie temperature T_c falls much more rapidly with decreasing x. There is no sign of magnetic order below $x = 0.57$ based on Mössbauer spectra. In other words, chromium is much more effective in destroying the iron moment in $Cr_{1-x}Fe_x$ glasses than in the crystalline phase. As far as we know, there has been no study done on the chromium-rich side of the same amorphous system.

In the present study, we report for the first time the transport data obtained for the $Cr_{1-x}Fe_x$ binary amorphous alloys. These alloys have a considerable advantage over the amorphous CrFe stabilized by metalloid atoms, because it is not clear how the valence electrons of metalloids contribute to the transport properties. Therefore, metal–metal amorphous alloys are more suitable candidates for investigating the influence of the magnetic state on low-temperature resistivity behaviour, since the magnetic order may be progressively suppressed without significant changes in structure.

0953-8984/96/5011121+10$19.50

The study has been carried out on $Cr_{0.824}Fe_{0.176}$, $Cr_{0.78}Fe_{0.22}$ and $Cr_{0.74}Fe_{0.26}$ amorphous thin-film alloys which correspond to spin glasses, and re-entrant and ferromagnetic phases for the crystalline counterparts, respectively.

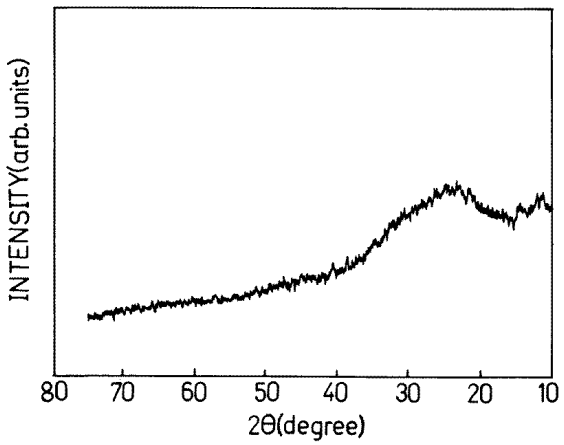

Figure 1. X-ray diffraction spectra of $Cr_{0.74}Fe_{0.26}$.

2. Experimental results

The flash-evaporation method was employed to obtain an amorphous alloy in the form of a thin film. First, the alloy ingots were prepared by melting together high-purity constituents in a rf furnace. Then, those ingots were filed into fine powders, which were slowly and continuously fed onto a preheated tungsten heater under a vacuum of 10^{-5} Torr. The films deposited onto a Corning glass substrate were held at room temperature. The four contact pads were prepared by evaporating a few nm of Au film through a photoresist lift-off mask. A lift-off mask was also used to pattern the sample size to typically 2.5 by 9 mm^2. The thickness was measured with the interferometric technique. The thicknesses of these films are 2850 Å, 2200 Å, and 3200 Å, respectively for $Cr_{0.824}Fe_{0.176}$, $Cr_{0.78}Fe_{0.22}$, and $Cr_{0.76}Fe_{0.26}$. The amorphous phase was confirmed in these films by ordinary x-ray diffraction. The scattering x-ray patterns showed no Bragg peaks but were characterized by a broad structureless intensity with a maximum at low angles characteristic of the amorphous state (see figure 1).

Resistivity measurements were carried out by using a conventional four-probe DC technique as a function of temperature between 1.5 and 300 K. The voltage accuracy was 1 in 10^5 and the current was maintained constant to 1 in 10^5 as well. Thus the values of the resistivities were given with maximum accuracy of 20% due to the uncertainty of the film dimensions. A calibrated Pt thermometer was used to measure the temperature between 4.2–300 K, and the temperatures below 4.2 K were obtained by pumping with vapour of liquid He. The temperature control was maintained with a cartesian monostat. The vapour pressure was monitored with an electronic manometer (CGS Scientific Co., Type 1018), and the monitored vapour pressures were converted to temperatures by means of the 1958 T-scale. The magnetoresistance measurements were performed by using an AC technique. Here, the voltage accuracy was better than one part in 10^7. The magnetic field (0–16 T) was supplied using a superconducting magnet. As for the magnetization measurements, we

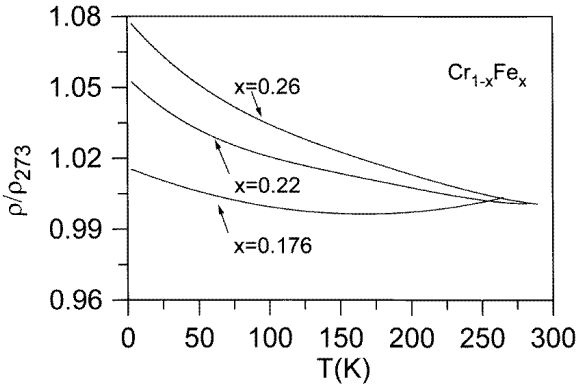

Figure 2. The temperature dependence of the electrical resistivity normalized to that at 273 K for $Cr_{1-x}Fe_x$ ($x = 0.176$, 0.22 and 0.26).

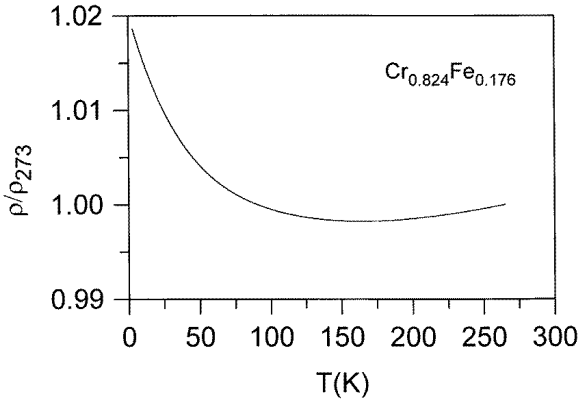

Figure 3. The temperature dependence of the resistivity normalized to that at 273 K for $Cr_{0.824}Fe_{0.176}$.

used a homemade magnetometer working in the temperature range of 1.5–200 K and in the magnetic field 0–7 T. The accuracy was better than 10^{-5} emu. The temperature was monitored and controlled via a carbon-glass thermometer to within an estimated accuracy of 0.01 K below 40 K and 0.05 K above 100 K.

Table 1. The resistivity at $T = 273$ K, the temperature cofficient ($B = -\Delta(\rho/\rho_0)\sqrt{T}$) and the magnetic state for $Cr_{0.824}Fe_{0.176}$, $Cr_{0.78}Fe_{0.22}$ and $Cr_{0.74}Fe_{0.26}$ are given.

Sample	ρ(273 K) ($\mu\Omega$ cm)	$B \times 10^{-3}$
$Cr_{0.824}Fe_{0.176}$	725	2.45
$Cr_{0.78}Fe_{0.22}$	1200	3.60
$Cr_{0.74}Fe_{0.26}$	1350	5.30

Shown in figure 2 are the resistivities normalized to their values at $T = 273$ K for the amorphous $Cr_{1-x}Fe_x$ ($x = 0.176$, 0.22, and 0.26) alloys as functions of temperature between

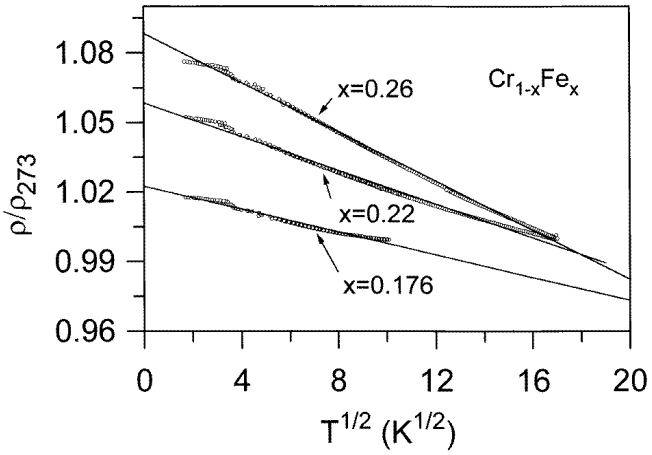

Figure 4. The temperature dependence of the resistivity with respect to that at 273 K on a square-root scale for $Cr_{1-x}Fe_x$: $x = 0.176$, 0.22 and 0.26.

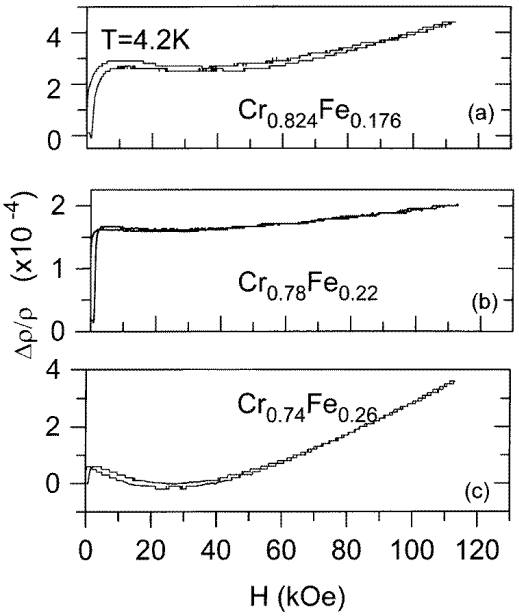

Figure 5. The longitudinal magnetoresistance at $T = 4.2$ K (a) for $Cr_{0.824}Fe_{0.176}$, (b) for $Cr_{0.78}Fe_{0.22}$ and (c) for $Cr_{0.74}Fe_{0.26}$.

1.5 K and 273 K. It can be seen that the sample with Fe content $x = 0.176$ exhibits a shallow minimum at around $T = 150$ K. In order to see this minimum more clearly, the normalized resistivity for this sample is also displayed in figure 3. The resistivity for the other samples probably passes through a minimum at higher temperatures which are above our temperature limit. The smooth increase of ρ for all samples below the temperature minimum is followed at lower temperatures by a stronger upwards curvature which is characteristic of many

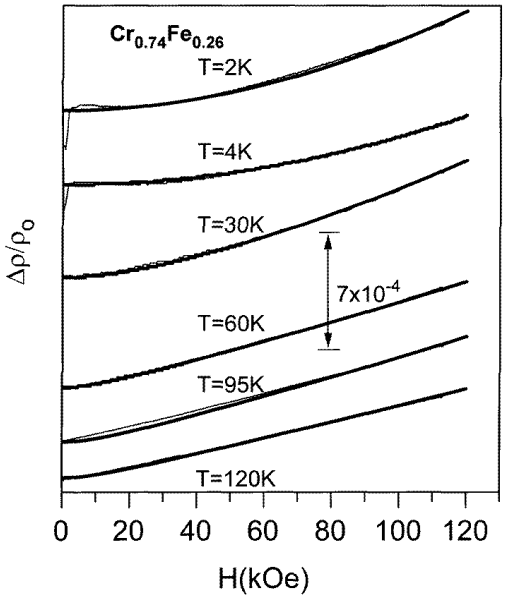

Figure 6. The longitudinal magnetoresistance of $Cr_{0.74}Fe_{0.26}$ at some selected temperatures. Note that the continuous thin lines show the experimental data, while the thick lines show the corresponding theoretical ones.

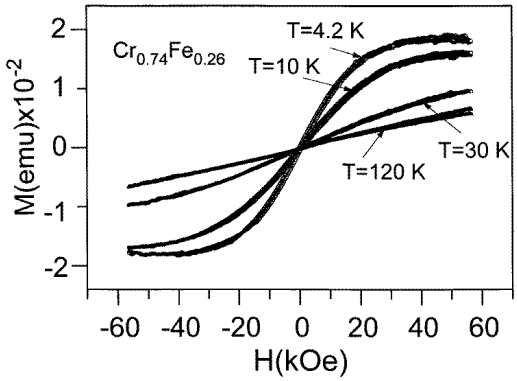

Figure 7. The magnetization curves of $Cr_{0.74}Fe_{0.26}$ for parallel geometry (the magnetic field parallel to the film surface) at selected temperatures. Note that the magnetization at $T = 4$–10 K saturates at about $H = 40$ kOe.

metallic glasses. To analyse our experimental data in terms of recent predictions for metallic glasses from interaction theories, the resistivities have also been plotted in figure 4 versus the square root of temperature ($\sqrt{T}$). The temperature coefficients, and the resistivities at $T = 273$ K are summarized in table 1. It should be noted that the temperature coefficients are directly correlated with the increasing of ρ and the decreasing of the magnetization M. To illustrate the ferromagnetic state of these samples, the magnetoresistance (MR) of each sample for parallel geometry (the current $\boldsymbol{J}$ parallel to the applied field $\boldsymbol{H}$) at $T = 4.2$ K is given in figure 5. As can be seen in these figures, the ferromagnetic anisotropy of the

resistivity (FAR) associated with domain rotation decreases with increasing Fe content. This means that the average magnetization over the scale of the mean free path of the conduction electrons (a few tenths of an ångström) decreases with Fe content. The magnetoresistance of $Cr_{0.74}Fe_{0.26}$ for some selected temperatures is also depicted in figure 6; we see that the magnetoresistance above $T = 10$ K is isotropic (i.e., it does not depend on the orientation of the field with respect to the film), while it is anisotropic at the lowest temperatures due to domain rotation. In the ferromagnetic (or superparamagnetic) regime, $\Delta\rho/\rho$ first increase rapidly at low fields due to the FAR, goes through a maximum, and then starts to decrease due to the decrease in the spin fluctuations associated with the d electrons. This behaviour is in good agreement with the magnetization curves (see figure 7). However, as the magnetic field is further increased, the magnetoresistance starts to increase again, but smoothly. A possible mechanism for this extra contribution may be that of weak localization. The macroscopic magnetization measurements of these films up to 60 kOe were also carried out by means of a vibrating-sample magnetometer in the temperature range 4–100 K. No distinct difference between the M versus H dependences for all three films has been detected, except in their technical saturation magnetization values. However, we have avoided giving the absolute values of M due to the uncertainty of the mass used for measurements. Figure 7 shows M versus H for the film $Cr_{0.74}Fe_{0.26}$ (the least magnetic among the samples) for some selected temperatures. The magnetization curves suggest that the Curie temperature T_c of this film is somewhere between 4.2–10 K. It should be noted that the magnetization at $T = 4$ and 10 K saturates at about 40 kOe (the demagnetization field for this geometry is almost zero). According to this behaviour, the magnetic structure of these amorphous alloys in the demagnetized state is thought to consist of a number of domains (or clusters) oriented randomly along with a rather strong magnetic anisotropy field. We will discuss this subject again below.

3. Discussion

We have shown that the temperature dependence of the above minimum exhibits a square-root temperature dependence. In the literature, two major possibilities have been suggested to explain the $-\sqrt{T}$-dependence of the resistivity at low temperatures. One of them is the localization theory (WL) [6, 7] and the other is the electron–electron (e–e) interaction theory [8, 9]. The two theories predict similar behaviour for the temperature dependences of the resistivity, but for the MR the predictions are quite different; the localization phenomenon gives either a negative magnetoresistance or a positive magnetoresistance in the case of the presence of strong spin–orbit scattering (or spin splitting from interactions), while the interaction theory shows a positive magnetoresistance. On the other hand, some authors [10, 11] suggest that if an amorphous alloy contains atoms with a magnetic moment, weak localization will be destroyed by magnons. Indeed, a recent study [12] show that the exchange enhancement plays dominant role in the magnetoresistivity. These effects incorporate into both weak localization and electron–electron interactions in some ways. Trudeau and Cochrane [12] first considered these effects properly for amorphous paramagnetic Zr–Fe. Furthermore, in the presence of strong spin–orbit interactions, Bieri *et al* [13] showed that the e–e interaction does not give a significant contribution to the magnetoresistance compared with that of the WL effects. We have obtained the magnetoresistivity data for our samples with these considerations in mind.

Fukuyama and Hoshino [14] first derived a general expression based on WL in analysing the magnetoresistance data. Then, Baxter *et al* [15] extended it to include the effect of scattering from magnetic impurities. We also used this expression in analysing our samples,

in order to account for the combined effects of Zeeman splitting and spin–orbit scattering together with magnetic spin-flip scattering. The contributions to magnetoresistance in our samples that need to be considered are as follows:

$$\left[\frac{\delta\rho}{\rho^2}\right]_{WL} = \frac{e^2}{2\pi^2\bar{h}}\sqrt{\frac{eB}{\bar{h}}}\left[\frac{1}{2\sqrt{1-\gamma}}\left\{f_3\left(\frac{B}{B_-}\right) - f_3\left(\frac{B}{B_+}\right)\right\} - f_3\left(\frac{B}{B_2}\right) - \sqrt{\frac{4B_{so}}{3B}}\left[\frac{1}{\sqrt{1-\gamma}}(\sqrt{t_+} - \sqrt{t_-}) + \sqrt{t} - \sqrt{t+1}\right]\right] \tag{1}$$

where

$$t = \frac{3B_\phi}{4(B_{so} - B_s)} \qquad t_\pm = t + \frac{1}{2}(1 \pm \sqrt{1-\gamma})$$

$$B_\pm = B_\phi + \frac{2}{3}(B_{so} - B_s)(1 \pm \sqrt{1-\gamma}) + 2B_s$$

$$B_2 = B_i + \frac{2}{3}B_s + \frac{4}{3}B_{so} \qquad B_\phi = B_i + 2B_s \qquad \gamma = \left(\frac{3g^*\mu_B B}{8eD(B_{so} - B_s)}\right)^2$$

where D is the electronic diffusivity and the characteristic fields are related to characteristic electron scattering times through relations of the type $B_x = \bar{h}/4eD\tau_x$ where $x =$ i, so, and s refer to the inelastic, spin–orbit, and magnetic spin-flip scattering times respectively. $f_3(x)$ is the Kawabata function [16] for a 3D disordered system.

Table 2. The fitting parameter $\gamma_{\text{eff}} = \gamma/(1-I)^2$.

T (K)	2	4	30	60	95	120
$1/(1-I)^2$	12	12	2.8	1	1	1

The calculation of the above expression (equation (1)) as a function of the magnetic field was performed on a Prime computer. We wrote a program by which the computed and measured curves can be displayed on the screen for comparison. The program can be used interactively when the user adjusts the parameters to obtain the best fit between theory and experiment. The data for $Cr_{0.74}Fe_{0.26}$ were fitted to the above expression for $0 \leqslant H \leqslant 120$ kOe and 4.2 K $\leqslant T \leqslant$ 120 K. Thus the overall best fit is obtained with a compromise as regards the values B_i, B_s, and B_{so} (see figure 7). In the ferromagnetic (or superparamagnetic) regime, we also need to use $\gamma_{eff} = \gamma/(1-I)^2$ rather than just γ to obtain the best fit. Here $1/(1-I)$ is the Stoner enhancement factor. The fitting values of γ_{eff} are summarized in table 2.

The theoretical analysis of $\Delta\rho/\rho$ versus H gives the characteristic fields B_x of the conduction electrons such as B_i, B_{so}, and B_s. Using the formulae

$$B_x\tau_x = \frac{\bar{h}e\rho N}{4} \qquad \frac{1}{\rho} = Ne^2D \tag{2}$$

one may calculate from the characteristic fields the corresponding characteristic times ($\rho =$ resistivity and $N =$ density of states at the Fermi energy for both spin directions). The diffusion coefficient D for all samples was taken as $\sim 10^{-4}$ m^2 s^{-1}. Other workers used a similar coefficient in other transition metal systems, such as Zr–M (M = Ni, Co, and Fe) [17], YAl [18], CuZr [19], and CuTi [20]. We obtain from curve fitting the spin–orbit scattering time $\tau_{so} \simeq 8 \times 10^{-15}$ s and the results for $\tau_i(T)$ and $\tau_s(T)$ are shown in figure 8. The spin–orbit scattering time τ_{so} could be determined from the critical fields at which the

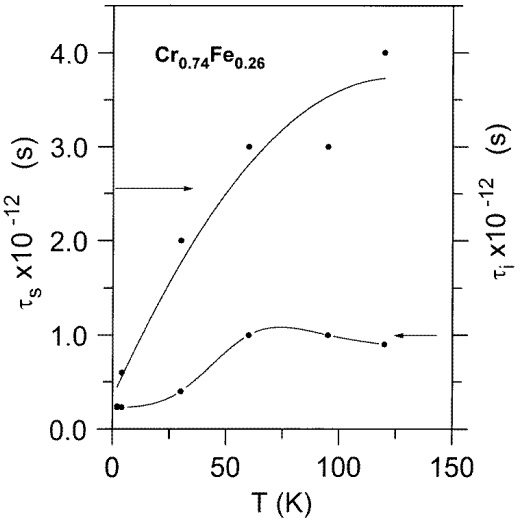

Figure 8. The inelastic scattering time τ_i and the spin-flip scattering time τ_s as functions of temperature for $Cr_{0.74}Fe_{0.26}$.

magnetoresistance vanishes [13], but $\Delta\rho$ for CrFe films still continues to increase at our highest fields ($\sim$12 T). This behaviour suggests that τ_{so} should be very strong. Indeed, non-superconducting Lu-based glasses [21] which exhibit a magnetoresistance behaviour similar to that of our system give $\tau_{so} \sim 10^{-14}$ s, in good agreement with our present finding. The large value of τ_{so} may be attributed to a strong spin–orbit scattering on the Fe sites. As for the inelastic scattering time τ_i, it remains almost constant throughout our temperature range. The order of the value of τ_i ($\sim 10^{-12}$ s) is in accord also with that observed for other transition metal system [13, 17–20]. The inelastic scattering rate presumably arises from electron–phonon scattering processes and remains of almost the same order at lower temperatures. This prediction seems to be reasonable due to the fact that the CrFe system is highly disordered and the localization phenomenon starts to occur at about room temperature. On the other hand, the spin-scattering times τ_s increase linearly with increasing temperature and then level off at about 50 K. This shows that the temperature dependence of the resistivity below 50 K is mainly determined by the temperature dependence of the spin fluctuation. Moreover, at much lower temperatures we need to take the exchange enhancement into account for the best fit. Trudeau and Cochrane [12, 17] first introduced the Stoner factor to account for their magnetoresistivity data on the paramagnetic amorphous Zr–Fe alloys. More recently, Bergmann and Beckmann [22] showed that weak localization is an excellent tool for investigating local spin fluctuations. They also pointed out that these fluctuations are enhanced by the Stoner factor due to the exchange interaction. Since these fluctuations like the spin–orbit scattering processes manifest themselves as a delocalization effect, we may expect to observe an increase in resistivity coefficient as the magnetization decreases. This is what we have seen in the resistivity of the CrFe system (see figures 2 and 4). We believe that localization and delocalization coexist even in the ferromagnetic regime for our highly disordered CrFe system.

We want to discuss the possible magnetic states pertaining to this amorphous system. Many authors [5, 23] have claimed that the disappearance of magnetism in the FeCrB system arises from the hybridization of Cr and Fe 3d orbitals of states, taking no sizable

charge transfer from Cr to Fe into account. The average zero hyperfine field on the iron has been taken as evidence for the destroying of the iron moment in FeCr glasses. It is also important to point out that the iron content is decreased, while the magnetization increases, in contrast to our expectation. Xia *et al* [24] recently obtained a pure amorphous phase in $Cr_{1-x}Fe_x$ alloy film ($0.25 \leqslant x \leqslant 0.60$) by thermal evaporation, using a very low deposition rate. They also showed by Mössbauer measurements that, at room temperature, the hyperfine field $\langle H_{hf} \rangle$ almost vanishes in the composition range $0.25 < x < 0.60$ for these films. However, it is still an open question whether Fe possesses a magnetic moment. A complete description of the magnetic structure of such a system requires a knowledge of the distribution in magnitude and orientation of the individual atomic moments. In fact, the average atomic moment can be deduced experimentally from the average hyperfine field or by neutron diffraction. But the relative orientations of the moments are more difficult to measure. On the other hand, the electrical resistivity is sensitive to the properties of a system roughly on a length scale less than the mean free path of the electrons in the alloys. For amorphous systems, this length is quite short, and provides a useful probe for studying the short-range behaviour in these alloys. In the light of the above discussion and taking into account the fact that the mean free path of conduction electrons (5–10 Å) is comparable with the interatomic distances, we therefore emphasize that Fe atoms must have magnetic moments even at room temperature unless the structure transition occurs below $T = 300$ K. Although the macroscopic magnetization is almost zero up to 7 T (our highest available field) at temperatures above $T = 50$ K, the vanishing of $\langle H_{hf} \rangle$ can be due to the local spin fluctuations.

4. Conclusion

We have studied the temperature dependence of the electrical resistivity of $Cr_{1-x}Fe_x$ ($x = 0.176$, 0.22 and 0.26) metallic glasses in the range 1.5–300 K. We have also carried out magnetization and the magnetoresistivity measurements on the same samples. We have analysed the magnetoresistivity data using the well-known Fukuyama and Hoshino expression extended to magnetic materials by Baxter *et al* [15] for the localization. Taking into account the local spin-fluctuation effects in addition to the strong spin–orbit effects, we have seen that the electrical transport mechanism for the CrFe system can be explained only by the localization. We have obtained the inelastic and spin-flip scattering rates as functions of the temperature. At low temperatures, local spin fluctuations play a predominant role in the temperature behaviour of the resistivity in agreement with the prediction of the model of Bergmann and Beckmann [22]. We can conclude that the spin–orbit scattering and spin-flip scattering due to the local spin fluctuations must be strong, yielding antilocalization. Therefore, the elastic and all of the inelastic scattering processes cannot be treated independently. Our conclusion is in disagreement with the work of Altounian *et al* [25] who have analysed their data for the $Fe_xNi_{1-x}Zr_2$ system by considering the resistivity due to the local spin fluctuations to be simply additive.

Acknowledgments

This research was supported by NATO (Project No: RCG 940539) and by the Scientific and Technical Research Council of Turkey (TBAG Project No: 1365). The support of one of us (AK) by a TBAG-TUBITAK grant is gratefully acknowledged.

References

[1] Burke S K, Cywinski R, Davis J R and Rainford B D 1983 *J. Phys. F: Met. Phys.* **13** 451
[2] Vind Nielsen H J 1979 *J. Magn. Magn. Mater.* **12** 187
[3] Yeshurun Y, Rao K V, Salamon M B and Chen H S 1981 *Solid State Commun.* **38** 371
[4] Olivier M, Strom-Olsen J O, Altounian Z and Williams G 1982 *J. Appl. Phys.* **53** 7696
[5] Yu Boliang, Coey J M D, Olivier M and Strom-Olsen J O 1984 *J. Appl. Phys.* **55** 1748
[6] Abrahams E, Anderson P W, Licciardello D C and Ramakrishan T V 1979 *Phys. Rev. Lett.* **42** 673
[7] A review of the weak-localization corrections to the conductivity is given by Bergmann G 1984 *Phys. Rep.* **107** 1
[8] Altshuler B L and Aronov A G 1979 *Zh. Eksp. Teor. Fiz.* **77** 2028 (Engl. Transl. 1979 *Sov. Phys.–JETP* **50** 968)
[9] A detailed review of Coulombic interaction corrections to the conductivity is given by Lee P A and Ramakrishan T V 1985 *Rev. Mod. Phys.* **57** 287
[10] Lee P A 1980 *J. Non-Cryst. Solids* **35** 21
[11] Altshuler B L, Khmelnitskii D, Larkin A I and Lee P A 1980 *Phys. Rev.* B **22** 5142
[12] Trudeau M L and Cochrane R W 1988 *Phys. Rev.* B **38** 5353
[13] Bieri J B, Fert A, Creuzet G and Ousset J C 1984 *J. Appl. Phys.* **55** 1948
[14] Fukuyama H and Hoshino K 1981 *J. Phys. Soc. Japan* **50** 2131
[15] Baxter D V, Richter R, Trudeau M L, Cochrane R W and Strom-Olsen J O 1989 *J. Physique* **50** 1673
[16] Kawabata A 1980 *Solid State Commun.* **34** 431
[17] Trudeau M L and Cochrane R W 1990 *Phys. Rev.* B **41** 10 535
[18] Olivier M, Strom-Olsen J O, Altounian Z, Cochrane R W and Trudeau M 1986 *Phys. Rev.* B **33** 2799
[19] Poon S J, Cotts E J and Wong K M 1984 *Solid State Commun.* **52** 519
[20] Howson M A and Greig D 1986 *J. Phys. F: Met. Phys.* **16** 989
[21] Poon J S, Wong K M and Drehman A J 1985 *Phys. Rev.* B **31** 1668
[22] Bergmann G and Beckmann H 1995 *Phys. Rev.* B **52** R15 687
[23] Dey S, Gorres U, Nielsen H J V, Rosenberg M and Sostarich M 1980 *J. Physique Coll.* **41** C8 678
[24] Xia S K, Baggio-Saitovitch E and Larica C 1994 *Phys. Rev.* B **49** 927
[25] Altounian Z, Dantu S V and Dikeakos M 1994 *Phys. Rev.* B **49** 8621